Published in final edited form as:
Biochemistry. 2009 December 15; 48(49): 11622–11629. doi:10.1021/bi901590q.

Insight into the mechanism of inactivation of ribonucleotide reductase by gemcitabine 5′-diphosphate in the presence or absence of reductant†

Erin Artin[‡], **Jun Wang**[§], **Gregory J. S. Lohman**[§], **Kenichi Yokoyama**[§], **Guixue Yu**[§], **Robert G. Griffin**[§], **Galit Bar**[§], and **JoAnne Stubbe**[*,§,‖]
Departments of Chemistry and of Biology, Massachusetts Institute of Technology, Cambridge, MA 02139

[‡]Intelligent BioSystems, 34 Bear Hill Road, Waltham, MA 02451

[§]Department of Chemistry, Massachusetts Institute of Technology.

[‖]Department of Biology, Massachusetts Institute of Technology.

Abstract

Gemcitabine 5′-diphosphate (F_2CDP) is a potent inhibitor of ribonucleotide reductases (RNRs), enzymes that convert nucleotides (NDPs) to deoxynucleotides and are essential for DNA replication and repair. The *E. coli* RNR, an α2β2 complex, when incubated with one equivalent of F_2CDP catalyzes the release of two fluorides and cytosine concomitant with enzyme inactivation. In the presence of reductant (thioredoxin/thioredoxin reductase/NADPH or DTT), the enzyme inactivation results from its covalent labeling of α with the sugar of F_2CDP (one-label/α2β2). SDS PAGE analysis of the inactivated RNR without boiling of the sample reveals that α migrates as an 87 kDa and 110 kDa protein in a ratio of 0.6:0.4. When the reductant is omitted, RNR is inactivated by loss of the essential tyrosyl radical and formation of a new radical. Inactivation studies with C225S-α in the presence or absence of reductants, reveal it behaves like wt-RNR in the absence of reductant. Inactivated C225S-α migrates as an 87 kDa protein and is not covalently modified. C225 is one of the cysteines in RNR's active site that supplies reducing equivalents to make dNDPs. To identify the new radical formed, [1′-^{2}H] F_2CDP was studied with wt- and C225S-RNR by 9 and 140 GHz EPR spectroscopy. These studies revealed that the new radical is nucleotide derived with g values of g_x 2.00738, g_y 2.00592, g_z 2.00230 and with altered hyperfine interactions (apparent triplet collapsed to a doublet) relative to [1′-^{1}H] F_2CDP. The EPR features are very similar to those we recently reported for the nucleotide radical generated with CDP and E441Q-RNR.

2′, 2′-Difluorodeoxycytidine (F_2C or gemcitabine) is used clinically in the treatment of non-small cell lung and pancreatic cancers (1-5). Its biological activity results from its inhibitory action on multiple steps required for DNA biosynthesis. F_2C is transported into the cell via three nucleoside transporters (ENT1, ENT2 and CNT1). It is then phosphorylated by human deoxycytidine kinase (hdCK) to the 5′-monophosphate (F_2CMP) and to the diphosphate (F_2CDP) by human UMP-CMP kinase (hCMPK) (6-8). Conversion to the triphosphate (F_2CTP) is most likely carried out by nucleoside diphosphate kinases (9). F_2CTP is believed to be the major cause of apoptosis in treated malignant cells, exerting its effect by its

†This work was supported by NIH grants (GM29595 to J.S. and EB-002804 and EB-002026 to R.G.G.

* To whom correspondence should be addressed. Tel: (617) 253-1814. Fax: (617) 258-7247. stubbe@mit.edu .

incorporation into DNA where it causes stalling of DNA synthesis and DNA chain termination (2). This mode of action is potentiated by the ability of F_2CDP to inhibit human ribonucleotide reductase (hRNR), the enzyme responsible for the conversion of nucleoside diphosphates to deoxynucleoside diphosphates (dNDPs) (10,11). This inhibition depletes levels of all dNDPs, and consequently dNTPs, in the cell and enhances the ability of F_2CTP to compete with dCTP for incorporation into DNA (12,13). Furthermore, depletion of dCTP releases the tight feedback inhibition of hdCK by dCTP and results in elevated levels of F_2CDP and F_2CTP (14). The ability of F_2C to affect its own metabolism is likely responsible for its unique cytotoxic properties relative to other nucleosides. The detailed understanding of the mechanism of inhibition of RNR by F_2CDP and the mechanism(s) for resistance to F_2C by overexpression of each of the subunits of RNR, α or β, associated with different cancers are active areas to research (4,5). This paper reports new insight into the mechanism of inhibition of *E. coli* RNR, a model for the hRNR, under conditions in which reductant is absent. A model for the inactivation process that accommodates available data is proposed.

Inhibition of RNR by nucleotides of F_2C has been most extensively studied with enzymes from *E. coli* and *Lactobacillus leichmannii* (15-17). The *E. coli* RNR is composed of two subunits α and β. The active site for nucleotide reduction is in α2 which is structurally homologous to the α of the *L. leichmannii* RNR, which is a monomer. The β2 subunit of *E. coli* RNR houses the diferric-tyrosyl radical (Y•) which initiates nucleotide reduction on α, while adenosylcobalamin initiates nucleotide reduction in the *L. leichmannii* RNR. The studies on the *E. coli* RNR revealed that the mechanism of inhibition by F_2CDP is reductant-dependent (15). In the presence of a reducing system, thioredoxin/thioredoxin reductase/ NADPH (TR/TRR/NADPH) or 1, 4-dithiothreitol (DTT), inhibition resulted predominantly from covalent labeling of α (1 label/ α2) (18). This labeling was accompanied by increased interaction between the two subunits, such that they migrated as an α2β2 complex by size exclusion chromatography. In the absence of reductant, inhibition resulted predominantly from the loss of the essential Y• located on β2. The Y• loss was accompanied by formation of a “new” stable radical (15). The structure of the new radical, which displays a triplet EPR lineshape at 9 GHz, was proposed to arise from interactions with two $I = ½$ nuclei. However, EPR spectra recorded in ^2H_2O and with uniformly deuterated α revealed no changes in the hyperfine interactions of the new radical. In addition, initial quantitative analysis of two products accompanying RNR inactivation in the presence and in the absence of reductant suggested that two equivalents (eq.) of fluoride and one eq. of cytosine per α2β2 were generated. No mechanistic models for inactivation were proposed at that time. More recently theoretical studies of Ramos and coworkers have resulted in proposed mechanisms for inactivation in the presence and absence of reductant (19,20).

Our initial studies were carried out with *E. coli* RNR (15 μM) and unlabeled F_2CDP. Using methods we have recently developed to incorporate labels into F_2CDP (^{3}H and ^{2}H at C1′, ^{3}H at C5 and ^{2}H at C3′), we now report inactivation studies in the presence and absence of reductants with 3 μM wt- and C225S-RNR. C225 is one of the five essential cysteines in α and its function is to supply the reducing equivalents to make dNDPs concomitant with its oxidation to a disulfide with C462 (21,22). We show that under physiological conditions, that is, with reducing equivalents available, covalent modification of α2 requires C225. C225S-RNR and F_2CDP in the presence or absence of reductant acts like wt RNR in the absence of reductant. The new radical generated by both wt and C225S RNR under these conditions is shown to be nucleotide based, as its production with [1′-^{2}H] F_2CDP results in collapse of the 9 GHz triplet hyperfine pattern to a doublet. EPR spectra of the radical at 140 GHz have provided the g-values of the new species. The radical produced has properties very similar to the radical generated when E441Q RNR is reacted with CDP and whose structure was recently established through isotopic labeling, ENDOR and EPR spectroscopy

and computational methods (23). A mechanism for the inactivation of RNR by F_2CDP in the absence of reductants and its relationship to inactivation in the presence of reductants is proposed.

MATERIALS AND METHODS

Triethylamine (99% pure) was purchased from Acros, and DTT from Mallinckrodt. [5-^{3}H]-F_2C (1 mCi, 14 Ci/mmol) was purchased from Moravek Biochemicals. All other materials were purchased from Sigma. F_2C was a gift from Eli Lilly and Company. [1′-^{2}H]-F_2C and [1′-^{3}H]-F_2CDP (specific activity (SA), 8261 cpm/nmol) were prepared as recently described (24,25). *E. coli* wt α2 was purified as described and had a SA of 1800–3000 nmol/mg/min. The concentration of α2 (dimer) was determined using ε (280nm) = 189 $mM^{-1}cm^{-1}$. α2 was pre-reduced as previously described (26). *E. coli* wt β2 and 6 × His-β2 (27) were isolated as described and had a SA of 6000–7000 nmol/mg/min. The concentration of β2 (dimer) was determined using ε (280nm) = 130.5 $mM^{-1}cm^{-1}$. The Y• content (1.1–1.2 Y•/ β2) was measured by the drop-line correction method and by EPR spectroscopy (28). *E. coli* thioredoxin (TR) was isolated from strain pTrx BL21 (DE3) and had a SA of 40 U/mg (29). *E. coli* thioredoxin reductase (TRR) was isolated from strain pMR14 K91 and had a SA of 1600 U/mg (30). *E. coli* C225S-α2 was purified as previously described (22). The clone for hdCK was the gift of Dr. Staffan Eriksson (The Biomedical Center, Uppsala, Sweden) (31) and that for the glutathione S-transferase fusion with human UMP/CMP kinase (hGST-CMPK) was a gift of Dr. Anna Karlsson (Huddinge University Hospital, Stockholm, Sweden) (8).

Time-dependent inactivation of α2 and β2 by F_2CDP in the presence or absence of reductants

In a final volume of 110 μL, a typical inactivation mixture contained: 1.6 mM ATP, 3 μM pre-reduced α2 (wt or mutant), 3 μM β2, 3, 6, or 15 μM F_2CDP, and no reductants, or reductants (5 mM DTT or 20 μM TR, 0.5 μM TRR, 1.0 mM NADPH) in 50 mM HEPES pH 7.6, 15 mM $MgSO_4$, 1 mM EDTA (Buffer A). All reactions were carried out at 25°C. Inhibition was initiated by the addition of F_2CDP and an aliquot of the reaction mixture was assayed before addition of F_2CDP for the zero time point. The assay was carried out by two methods. In method 1, a 5 μL aliquot was diluted ten fold into Buffer A to give final concentrations of 1.6 mM ATP, 0.3 μM α2, 0.3 μM β2, 1 mM CDP (or [^{3}H]-CDP, SA 4000 cpm/nmol), 20 μM TR, 0.5 μM TRR, and 0.2 mM NADPH. In method 2, a 5 μL aliquot was diluted 20 fold into 95 μL of Buffer A with a five fold excess of a second subunit to give final concentrations of 1.6 mM ATP, 0.15 μM α2 (β2), 0.75 μM β2 (α2), 1 mM CDP (or [^{14}C]-CDP, SA 3200–5000 cpm/nmol), 20 μM TR, 0.5 μM TRR, and 0.2 mM NADPH (1 mM NADPH for the radioactive assay). Deoxynucleotide production was monitored either using the spectrophotometric assay or the radioactive assay with analysis by the method of Steeper and Steuart (32).

Phosphorylation of [5-^{3}H]-F_2C to form [5-^{3}H]-F_2CMP

In a final volume of 5 mL, the reaction contained 1 mM [5-^{3}H]-F_2C (SA of 23000 cpm/nmol), 1.33 mg/mL 6×His-hdCK (SA 170 nmol /mg/ min), 2 mM ATP, 2 mM DTT, and 0.5 mg/mL BSA, in 50 mM Tris (pH 7.6), 100 mM KCl, 5 mM $MgCl_2$. The reaction was initiated by the addition enzyme and incubated at 37° C for 10 min. Anion-exchange purification of the monophosphate was carried out on a 15 mL DEAE A-25 Sephadex column (1×19 cm) with a 90 × 90 mL linear gradient from 0.005-0.4 M triethylammonium bicarbonate (TEAB) pH 7.5. Fractions of 9 mL were collected. Five μL of each fraction was analyzed for radioactivity in 10 mL of Emulsifier-Safe scintillation fluid (Packard) using a Beckman LS 6500 Scintillation Counter. Fractions 18-24 were pooled and excess TEAB

was removed in vacuo. The product was obtained in 93% yield quantitated by UV-Vis absorption (λ_{max} 271 nm, λ_{min} 249 nm).

Phosphorylation of [5-^{3}H]-F_2CMP to [5-^{3}H]-F_2CDP

The reaction contained in a final volume of 4.65 mL: 1 mM [5-^{3}H]-F_2CMP, 65 μg/mL h GST-CMPK (SA 4.8 μmol/mg/ min), 4 mM ATP, and 2 mM DTT in 50 mM Tris (pH 8.0), 5 mM $MgCl_2$. Reactions were initiated by addition of enzyme and incubated at 37 °C for 30 min. The diphosphate was purified by DEAE Sephadex A-25 chromatography (15 mL, 1×19 cm) using a 120 × 120 mL linear gradient of 5 mM to 0.6 M TEAB (pH 7.5). Fractions (6 mL) were collected and assayed by scintillation counting. Fractions 28-36 were pooled and the TEAB removed in vacuo. F_2CDP and ADP co-eluted and the ADP was removed subsequent to periodate oxidation. Sodium periodate (0.5 M) was added to a final concentration of 18.6 mM (4 eq. relative to starting [5-^{3}H]-F_2CMP). The mixture was incubated at 37 °C for 10 min and then 4 M methylamine was added to a final concentration of 100 mM and the mixture incubated at 37 °C for 20 min. The 4 M methylamine stock solution was freshly prepared from a 40% aqueous solution (Aldrich) and the pH was adjusted to 7.3 by the dropwise addition of 85% phosphoric acid with stirring on ice. The oxidative cleavage was quenched by the addition of L-rhamnose to a final concentration of 37.5 mM (8 eq. relative to starting [5-^{3}H]-F_2CMP) followed by incubation at 37 °C for 10 min. To remove the pyrophosphate generated during this process, the reaction was brought to 33 mM Tris (pH 7.2) by addition of 0.33 volumes of 100 mM Tris (pH 7.2) and incubated with 5 U/1.5 mL inorganic pyrophosphatase from Baker's yeast (E.C. 3.6.1.1, Sigma) in the presence of 1.6 mM $MgCl_2$ at 25 °C for 30 min. [5-^{3}H]-F_2CDP was purified on a 15 mL DEAE Sephadex A-25 column (1 × 19 cm) using a 120 ×120 mL linear gradient of 0.005 M to 0.6 M TEAB (pH 7.5). Fractions (6 mL) were collected and assayed by scintillation counting. Fractions 28-36 at 0.4 M TEAB were pooled and concentrated in vacuo to give 78% yield by UV absorption. ^{1}H NMR was acquired on a 500 MHz INOVA spectrometer from Varian. The spectrum was referenced to H_2O: NMR (D_2O, pH 5.6) δ 4.13 (m, 1H), 4.30 (m, 2H), 4.56 (m, 1H), 6.10 (d, J = 7.6 Hz, 1H), 6.20 (t, J = 7.0 Hz, 1H), 7.85 (d, J = 7.6 Hz, 1H). The ^{31}P NMR was acquired on a 300 MHz MERCURY spectrometer from Varian using 85% H_3PO_4 in water as the external standard: ^{31}P NMR (D_2O, pH 5.6) δ –10.08 (d, J = 20.4 Hz, 1P), –5.95 (d, J = 20.0 Hz, 1P).

Synthesis of [1′-^{3}H]-F_2CDP and [1′-^{3}H] F_2CDP

[1′-^{2}H]-F_2C (90% 1′-^{2}H and a 60:40 mixture of α:β anomers) and [1′-^{3}H]-F_2C (SA 8700 cpm/nmol) were converted to the monophosphate and then diphosphate as described above.

Covalent modification of wt-RNR and C225S-RNR with [1′-^{3}H]-F_2CDP or [5-^{3}H]-F_2CDP

The reaction mixture contained in a final volume of 210 μL: 3 μM α2 (wt or mutant), 3 μM β2 (wt or 6 × His), 6 μM or 15 μM [5-^{3}H]-F_2CDP or [1′-^{3}H]-F_2CDP, 1.6 mM ATP, Buffer A and no reductant or reductant (either 5 mM DTT or 20 μM TR, 0.5 μM TRR, and 1.0 mM NADPH). All reaction components except for F_2CDP were mixed and equilibrated at 25°C for 5 min. A **5** μL aliquot of the reaction mixture was removed prior to inhibitor addition and at the end of 20 min and assayed for activity. Two hundred μL was then loaded directly onto a Sephadex G-50 column (1 × 25.5 cm) equilibrated in 50 mM HEPES pH 7.6. Fractions of 1 mL were collected. Aliquots of each fraction (500 μL) were assayed by scintillation counting and the protein quantitated by A_{280nm}.

Quantitation of cytosine released during the inactivation of E. coli RNR by [5-^{3}H]-F_2CDP

The reaction mixture contained in 750 μL: 3 μM α2 and β2 and 6 μM [5-^{3}H]-F_2CDP (6643 cpm/nmol, 2 eq./α2), 1.6 mM ATP, and 20 μM TR, 0.5 μM TRR, 1.0 mM NADPH in 50

mM HEPES pH 7.6, 15 mM $MgSO_4$, 1 mM EDTA. The reaction was incubated for 20 min at 25 °C. The mixture was then filtered through an YM-30 Centricon device (Millipore) at 4° C. F_2C (80 nmol) and cytosine (120 nmol) were added as carriers before filtration. The flow through was treated with 30 U of alkaline phosphatase (Roche) for 2 h at 37 °C and filtered through a second YM-30 Centricon device. The flow through was analyzed using a Waters 2480 HPLC with an Altech Adsorbosphere Nucleotide Nucleoside C-18 column (250 mm × 4.6 mm) at a flow rate of 1 mL/min. The elution buffer contained: Buffer I, 10 mM NH_4OAc, pH 6.8; Buffer II: 100% methanol. A 10 min isocratic elution with Buffer I was followed by a linear gradient to 40% buffer II over 30 min. A linear gradient was then run to 100% buffer II over 5 min. Fractions (1 mL) were collected and 200 μL of each were analyzed by scintillation counting. The recovery of [5-^{3}H]-cytosine and [5-^{3}H]-F_2C was calculated based on the UV spectrum (cytosine, $\lambda_{267\ nm}$, $\varepsilon = 6100\ M^{-1}cm^{-1}$, F_2C, $\lambda_{268\ nm}$, $\varepsilon = 9360\ M^{-1}cm^{-1}$) and normalized for carrier added. The radioactivity recovered with [5-^{3}H]-cytosine and [5-^{3}H]-F_2C was analyzed by scintillation counting.

Inactivation of RNR with F_2CDP monitored by 140 GHz EPR spectroscopy

A final volume of 15 μL contained: 1.6 mM ATP, 75 μM wt-α2, 75 μM β2, and 300 μM F_2CDP, in Buffer A at 25°C. The reaction was initiated by the addition of F_2CDP and aliquots were drawn into suprasil capillaries (silica, OD 0.55 mm, ID 0.4 mm, from Wilmad LabGlass) by capillary action. The samples were frozen in liquid N_2 at 30 s to 3 min after initiation.

Spectra were acquired at 60 K on a custom-designed pulsed spectrometer (33). Echo-detected spectra were acquired using a stimulated echo sequence with a pulse length of $t_{\pi/2}$ = 72 ns and a pulse spacing of τ = 230 ns or a pulse length of $t_{\pi/2}$ = 65 ns and a pulse spacing of τ = 200 ns. As previously demonstrated, the time domain approach allowed us to filter out the new radical from the Y• (34). The external magnetic field was swept with the assistance of a field lock described previously (34). The echo intensity at each field position was integrated, and an average of 1000 samples per point was taken.

9 GHz EPR experiments and simulations of the reaction of RNR and C225S-RNR with [1′-^{x}H]-F_2CDP (x = 1 or 2)

All reactions were carried out in a final volume of 230 μL and contained 15 μM α2, 15 μM β2, 75 μM F_2CDP, and 1.6 mM ATP in Buffer A at 25 °C. The reaction was initiated by the addition of F_2CDP and at 45 s, the reaction mixture was transferred into a calibrated 706 PQ EPR tube (Wilmad) and frozen in liquid N_2. EPR spectra were acquired on a Bruker ESP-300 spectrometer at 77 K. Spectra were acquired at 20 μW with 100 kHz modulation frequency, 1 G modulation amplitude, conversion time of 20.48 ms, and time constant of 5.12 ms. Typically, the sweep width was 150 G and 2048 points were acquired per spectrum. Simulations of the 9 GHz EPR spectra were performed with either SimFonia or EasySpin (35). The g-values determined from the 140 GHz spectra were: $g_x = 2.00738$, $g_y = 2.00592$, $g_z = 2.00230$. All spectra were simulated with a Lorentzian to Gaussian lineshape broadening ratio of 1. Parameters for the linewidth and the components of the hyperfine coupling tensor, A_{xx}, A_{yy}, A_{zz}, were varied to obtain the best fit.

Analysis of the reaction of wt- and C225S-RNR with F_2CDP by SDS PAGE

The inactivation mixture contained in a final volume of 50 μL: 5 μM α2 and β2, 3 mM ATP, with or without 5 mM DTT, and Buffer A. The reaction was initiated by addition of 2.5 eq. of F_2CDP (12.5 μM) and incubated at 25°C for 5 min. The inactivation mixture (8 μL) was mixed with 8 μL 2× loading buffer ± β-ME. The samples were either heated at 90 °C for 2 min or not heated before loading on a 10% SDS-PAGE gel. The proteins were visualized

with Coomassie blue staining. The band intensities were quantified using Quantity One software from Bio-Rad.

RESULTS

Time-dependent inactivation of RNR or C225S-RNR by F_2CDP

The assay for activity of *E. coli* RNR is unusual in that the two subunits have weak affinity for one another that is dependent on the presence of nucleotides. The K_d for subunit interaction with CDP/ATP is 0.2 μM (36). Typically the activity of each subunit is assayed independently by adding a large excess of the second subunit. A second complexity of the assay is that activity is not directly proportional to the concentration of enzyme. At higher enzyme concentrations for example, the rates of the reactions are typically slower (26). These complexities are likely associated with the coupled assay that requires re-reduction of the disulfide bond accompanying nucleotide reduction by TR/TRR/NADPH.

Time-dependent inactivation experiments of *E. coli* RNR by F_2CDP were initially carried out at 15 μM α2 and β2 using a five-fold molar excess of F_2CDP. To examine the stoichiometry of inactivation under physiological concentrations of RNR, the time-dependent inactivation studies were reexamined with α2 and β2 at 3 μM and F_2CDP at 3 μM in the absence of reductant. The assay was monitored in two ways. In method 1, the inactivation mixture was diluted 10-fold and assayed for dCDP production directly. Under these conditions (Figure 1A) the enzyme was completely inactivated with 1 F_2CDP/α2. In method 2 the inactivation mixture was diluted 20- fold with a 5 fold excess of the subunit not being assayed. Under these conditions β2 lost 90% of its activity associated with loss of the Y• (Figure 1B, red) and α2 lost 40% of its activity with some activity recovered with time (Figure 1B, blue). These results are very similar to the previous studies carried out at 15 μM RNR (15, 18) and also indicate that RNR is completely inactivated with one F_2CDP per α2β2.

Time-dependent inactivation of C225S-α2•β2 by F_2CDP

In our earlier experiments, C754S/C759S-α2β2 in the presence of TR/TRR/NADPH behaved like the wt-RNR in the absence of reductant, as judged by time-dependent inactivation of β2 and by detection of the new radical by EPR methods (15). C754 and C759 are located in the C-terminal tail of α2 and are responsible for re-reduction of the active site disulfide on each turnover (21). In the presence of DTT, a reductant that can re-reduce the active site directly, inactivation of C754S/C759S-α2β2 proceeded as with in wt-RNR in the presence of reductants, either TR/TRR/NADPH or DTT. These results together suggested that the mode of inactivation observed in the presence of reductants requires the delivery of reducing equivalents to the active site. This model further suggests that C225 and C462 may be oxidized during the inactivation process and that re-reduction of the disulfide may be necessary for the alkylation mode. Given this hypothesis, time-dependent inactivation of both subunits of C225S-α2β2 by F_2CDP (method 2, above) was monitored in the absence of reductant and in the presence of TR/TRR/NADPH or DTT. The results of activity assays for β2 under these conditions are shown in Figure 1C. Under all conditions, C225S-α2β2 exhibits a pattern of β2 inactivation that is characteristic of the wt-RNR in the absence of reductants (compare Figure 1C with Figure 1B, red).

C225S-α2β2 with [1′-^{3}H]-F_2CDP: Sephadex chromatography to monitor covalent labeling

If C225 is essential for inactivation by the alkylative pathway, then incubation of [1′-^{3}H]-F_2CDP with C225S-α2β2 should result in greatly reduced labeling relative to wt-RNR (1 eq. ^{3}H/α2) in the presence of reductant. When C225S-α2β2 was incubated with [1′-^{3}H]-F_2CDP in the presence of TR/TRR/NADPH and ATP, 0.14 eq. of the inhibitor were

associated with the protein under native conditions (average of two runs) and 0.15 eq. were associated under denaturing conditions. This data supports the proposal that C225 is required for the majority of labeling that occurs in the wt reaction in the presence of reductants.

SDS PAGE of RNR inactivated by F_2CDP in the presence and absence of reductant

Our recent studies on *L. leichmannii* RNR and human RNRs indicated that SDS PAGE analysis of the enzyme subsequent to its inactivation by F_2CTP (*L. leichmannii*) and F_2CDP (human) resulted in 35-50% of α migrating more slowly on the gel relative to the wt-α (24,25). This altered conformation of α appeared to be associated with the extent of covalent labeling by the sugar moiety from the inhibitor. A similar analysis was carried out on the *E. coli* RNR/F_2CDP reaction mixture in the presence and absence of reductant (Figure 2). Lanes 1-4 contain the inactivation mixture in the presence of the reductant DTT and Lanes 5-8 are identical to Lanes 1-4 without DTT. Lane 1 is the reaction mixture prior to addition of F_2CDP and Lane 4 shows the results when the sample is boiled prior to loading the gel. A slowly migrating band is observed in the presence of DTT and when the sample is loaded without boiling (Lanes 2 and 3, Figure 2). Appearance of this new band is associated with loss of α. We propose that this new species is an altered conformation of α that migrates like a protein of 110 kDa. Several pieces of evidence support this proposal. First, our recent mutagenesis studies with the human RNRs suggested that C218 (equivalent to C225 in the *E. coli* RNR) plays an important role in covalent modification of the enzyme (37). When C218S-hRNR and β or β' were inactivated by F_2CDP/ATP altered migration of α occurred in the presence or absence of DTT. Furthermore, boiling of the sample resulted in loss of its altered migratory properties as with *E. coli* RNR (37). Second, preliminary mass spectrometric analysis of a tryptic digest of this species with altered migratory properties, reveals that it is α (data not shown). Third, the adenosylcobalamin-dependent class II RNR that is a monomer homologous to α, shows altered migratory properties (24,25).

Cytosine production accompanies inactivation: use of [5-^{3}H] F_2CDP

Our previous studies with *E. coli* RNR (15 μM) and F_2CDP, and more recent studies with hRNR (5 μM) and [5-^{3}H] F_2CDP, both indicated that 0.5 eq. cytosine/α is produced during the inactivation (15,18). In this study, the experiments were repeated with *E. coli* RNR (3 μM). In the presence and absence of DTT, the amount of cytosine released was determined by HPLC and the amount retained with the protein was determined by Sephadex G50 chromatography. In the presence of DTT, the amount of cytosine released after a 20 min incubation was 0.85 eq./α and the amount of [^{3}H] associated with the protein was 0.08 eq. (average of 3 experiments). The remaining radioactivity was recovered as F_2C, subsequent to phosphate removal and accounted for mass balance. The amount of cytosine released is greater than previously reported from studies with higher enzyme concentrations (15 to 75 μM), although quantitation was more difficult as labeled F_2CDP was not available. Thus with 3 μM RNR and DTT, between 0.5 and 1 F_2CDP/α is required for complete inactivation.

In reactions carried out without DTT, the amount of cytosine determined varied from 0.1-0.15 eq./α (from 12 experiments) after a 20 min incubation, after the inactivation was complete. Analysis of radiolabel associated with the protein by Sephadex G50 chromatography gave 0.075 eq./α and when the chromatography was carried out with ATP in the eluent, 0.125 eq./α. When the same experiment was carried out after a five min incubation and the Sephadex chromatographic analysis was shortened to 12 min, only 0.08 eq./α was still associated with the protein. The small amounts of cytosine recovered with the protein in these experiments will be discussed subsequently. In contrast to the experiments carried out in the presence of reductant, the remainder of the radioactivity, subsequent to dephosphorylation migrated on a reverse phase HPLC column as a broad peak with retention

times similar to nucleoside analogs of cytidine. Analysis of these products would likely require their stabilization by $NaBH_4$ reduction as successfully carried out with *L. leichmannii* RNR inactivated by F_2CTP (24,25).

Structure of the New Radical at 140 GHz

In our previous studies of inactivation of RNR by F_2CDP in the absence of reductant, a new radical was generated concomitant with loss of the Y•. Forty percent of the Y• was lost on a rapid (30 s) time scale at 75 μM RNR. The analysis of the new radical was challenging at 9 GHz due to the spectral overlap between the new radical and the Y•. Our previous studies have demonstrated that high-field pulsed EPR at 140 GHz can be used to facilitate deconvolution of overlapping spectra (34). This method takes advantage of fact that the Y• is adjacent to a diferric cluster and thus its signal has an enhanced spin lattice relaxation time relative to that expected for the new radical which is located in α >35Å from the Y•. Thus analysis of the spectrum of the inactivation mixture at 60 K by this method gave the first clear view of the new radical (Figure 3) and allowed determination of its g-values (2.00738, 2.00592, 2.0023). The high-field spectrum and the g-values of the new radical are strikingly similar to those obtained of a radical derived from CDP when E441Q-α was incubated with TTP, DTT, and β (23). Extensive ENDOR, EPR, and computational studies in conjunction with isotopic labeling studies using [1′-^{2}H] and [4′-^{2}H] CDP, revealed the structure of this radical to be semidione nucleotide radical (**4**, Figure 4). Thus we propose that the structure of the new radical observed during the F_2CDP inactivation with no reductants is **4**.

EPR spectrum at 9 GHz of wt-RNR inactivated with [1′-^{2}H] F_2CDP

To obtain evidence in support of **4** (Figure 4) as the structure of the new radical, wt-RNR (15 μM) was incubated for 45 s with [1′-^{1}H]-F_2CDP/ATP, the sample was frozen in liquid N_2 and examined by 9 GHz EPR spectroscopy (Figure 5A, red). Subtraction of the Y• (Figure 5A, blue) from this spectrum gave the spectrum of the new radical (black). This spectrum is very similar to that we previously reported with 75 μM RNR (15). Under these conditions, within 45 s, 50 to 60% of the Y• was lost and 0.4 to 0.48 eq. of the new radical was observed. These values are higher than those previously reported due to the higher RNR concentrations used and the slower rates of inactivation in the previous studies. We have previously observed with mechanism based inhibitors that higher concentrations of RNR used to obtain EPR spectra, result in slower inactivation rates. The basis for the kinetic differences are not understood, but may be related to altered quaternary structure.

An identical experiment was then carried out with [1′-^{2}H]-F_2CDP with the results shown in Figure 5B. Subtraction of Y• (blue) resulted in the spectrum in black in which the apparent triplet (Figure 5A) has collapsed to a doublet. A similar experiment using [U-^{2}H]-β2 gave a spectrum similar to that in Figure 5A (data not shown). The amount of new radical formed was 80% that of the Y• lost, which suggests that 0.4 eq./α were generated. If **4** is indeed the structure of the new radical (Figure 4), then cytosine should be retained by the protein in an amount eq. to the amount of new radical. The cytosine co-migrating with protein, however, is lower (0.08) than expected based on the 0.25 vs 0.4 eq. of radical. It becomes closer (0.125 eq.) when the protein was chromatographed with ATP effector in the elution buffer. We will argue subsequently that this discrepancy is associated with the analytical method for cytosine recovery and hence we still favor the structure of **4** in Figure 4 for the new radical.

EPR spectrum at 9 GHz of C225S-RNR inactivated with [1′-^{2}H]-F_2CDP

C225S-α2β2 was incubated with [1′-^{1}H]-F_2CDP/ATP in the absence or presence of reductants (TR/TRR/NADPH or DTT). The time-dependent inactivation studies (Figure 1C) indicate that under all conditions that a new radical identical to that in Figure 5A should be

observed. Furthermore, with [1′-^{2}H]-F_2CDP, a collapse in the hyperfine structure would be expected. In the former case a triplet spectrum very similar to that shown in 5A was in fact observed (data not shown) and the results of the latter experiment are shown in Figure 5C. The serine mutant of C225 still allows the chemistry to occur to generate the new radical.

DISCUSSION

Phosphorylated gemcitabine is a stoichiometric mechanism-based inhibitor of class I and II ribonucleotide reductases (15,17). Despite the stoichiometry, however, the mechanism(s) of inactivation revealed by the current studies and our previous studies are very complex and involve multiple pathways. We have recently shown, for example that with the class I RNRs, both the *E. coli* and human enzymes, that inactivation with [1′-^{3}H] F_2CDP in the presence of reductants results in 0.5 labels/α and that it is due to increased affinity of the two subunits for one another relative to their affinity observed in the presence of the normal substrate/effector pairs (18).

Our past and current studies on *E. coli* and *L. leichmannii* RNRs have led to a model to account for the pathway of inactivation in the absence of reductant in which Y• is lost and a new, nucleotide-based radical is generated. Our working model is shown in Figure 4. In this model, the first step is 3′-hydrogen atom abstraction followed by loss of F^- (**1** to **3**, Figure 4). These steps are analogous to those suggested for the reaction of RNR with 2′-fluoro-2′-deoxynucleoside 5′-diphosphate where we showed that the enzyme catalyzes partitioning between inactivation through a 3′-ketodeoxynucleotide and ultimately furanone formation and deoxynucleotide formation based. The partitioning depended on the presence of reductant and differed with TR/TRR/NADPH and DTT (11,38). The next step in the model is that water attacks the 2′ carbon to generate **4** concomitant with loss of the second F^-. Intermediate **4** is proposed to be the new nucleotide radical detected by EPR spectroscopy. The conversion of **3** to **4**, to our knowledge, has no chemical precedent. This step is the reverse of water loss in the normal reduction process and requires that there is a water in the active site in the vicinity of the C2′ carbon. A similar mechanism for covalent modification of RNR by C225 (**5**,Figure 4) has been proposed by Ramos and coworkers based on DFT calculations (19) and previously by us (**5**,Figure 5). Unfortunately, the charges on the intermediate proposed in the Ramos model (12 in their Scheme 2) appear to be incorrect. Thus the kinetic “feasibility of nucleophilic attack at C2′ and its dependence on the nucleophile□, needs to be reexamined computationally. In our proposed mechanism (Figure 4), we have ignored the fate of the fluorides and the source of water. Our biochemical studies, however, have shown that both fluorides are lost, at different rates, and an X-ray structure of the *S. cerevisiae* α with F_2CDP and AMPNP (a nonhydrolysable analogue of ATP) soaked into the active site, suggests that waters are present on the bottom face of the nucleotide (39). The *S. cerevisiae* structure, if applicable to the *E. coli* RNR, also suggests that covalent modification of the sugar moiety derived from F_2CDP would likely be by C225. This cysteine and water are the only nucleophiles close to the sugar in the structure. E441, known to be essential for catalysis and located on the bottom face of the nucleotide, is displaced from its interaction with the 3′-OH of the nucleotide and thus is unlikely to be involved in covalent modification. Finally, as with all mechanism-based inhibitors (10), cytosine is eventually lost. This loss is usually associated with transformation of some intermediate (4 or 5, Figure 4) into a 3′-ketone that then slowly loses cytosine.

Several pieces of data from the present studies support the model in Figure 4. The first is that the new radical is nucleotide-based as it exhibits hyperfine interaction with the C-1′ proton consistent with **4**. The proposal of **4** as the new radical is also supported by our recent investigations of the mechanism by which E441Q-α in the presence of CDP, allosteric effector TTP and β2, results in Y• loss and formation of a new nucleotide radical derived

from CDP (23). Extensive isotope labeling experiments (including [4′-^{2}H] and [1′-^{2}H] CDP) in conjunction with ENDOR and EPR spectroscopy and computational analysis provided strong evidence that **4** is the structure generated. It should be noted, however, that the mechanism by which **4** is generated is not understood in either case and when derived from CDP and E441Q-α, must be distinct from when it derived from F_2CDP and α. In addition, recent studies on the inactivation of the *L. leichmannii* RNR by F_2CTP resulted in trapping of a cytidine analog thought to be derived from oxidation of radical **4** during $NaBH_4$ trapping (24). Finally a monofluorinated cytidine derivative (**3**,Figure 4) was also trapped with $NaBH_4$ with the C119S mutant (C225 equivalent in the *L. leichmannii* RNR) (24,25,38).

The mechanism (Figure 4) predicts that the new radical still has its cytosine moiety attached. Thus experiments with [5-^{3}H]-F_2CDP and isolation of RNR should reveal if the stoichiometry of the radical is equivalent to the amount of base residing with the protein. The analysis, however, is complicated for several reasons. The first is that the amount of the new radical is difficult to quantitate due to its spectral overlap with the Y•. Second, both radicals decay with time. Third, most experiments to look for cytosine release were all carried out subsequent to a 20 min incubation, while the new radical is formed within 45 s. The complete inactivation occurs over 20 min in which case the new radical is likely decomposing with loss of cytosine. Thus the observed value of 0.08-0.12 ^{3}H/α and the estimation of 0.4 new radicals/α, given the complications, suggest that base can still be attached to the new radical, consistent with **4**.

Finally, the studies with the C225S mutant support the proposed mechanism of inactivation in that no redox chemistry is involved in formation of the new radical and thus no reducing equivalents are required for inactivation involving loss of Y•. Furthermore, the studies with this mutant support the importance of C225 in the alkylative pathway (**5**), the one involving covalent modification of the protein. With the mutant, no label is attached to the protein despite the fact that this mutant can catalyze the first few steps in the pathway.

Our efforts to isolate and identify a peptide(s) labeled in the alkylative pathway have revealed that the alkylated product can rearrange during the work-up. Even efforts to trap the alkylated adduct(s), likely a ketone moiety or an α, β-unsaturated ketone, by reduction with $NaBH_4$, which should preclude rearrangements, have been unsuccessful. Similar studies on the hRNR have also been unsuccessful. Only in the case of the *L. leichmannii* RNR has a peptide, containing the C-terminal cysteines attached to a sugar derived from F_2CTP, been identified (24). Even in that case, however, the recovery of total label in that peptide relative to total label attached to the protein is low, indicating that other non-isolable adducts are also generated. Our inability to identify a site(s) of labeling is unusual given that the inactivation is stoichiometric. The difficulty is likely related to reorganization of furanone-like moieties, by reverse Michael additions, prior to trapping with reductant (11). The observation that C225S-α is labeled at 10% that of the wt-α, supports the role of C225 in alkylation, perhaps via cross-linking with a cysteine in the C-terminal tail of α. Finally the unusual observation made with all RNRs examined thus far is that accompanying their inactivation, an altered conformation of the α subunit is generated which migrates as 110 kDa protein by SDS PAGE (Figure 2). Recent crystallization of the complex of the *E. coli* RNR inactivated by F_2CDP and analysis of the crystals by SDS PAGE indicate the presence of this altered α structure (Stock, Drennan, unpublished results). We propose that C225 and a C-terminal cysteine are both bound to the sugar derived from F_2CDP during inactivation, causing a substantial change in the structure of α.

In the past few years we have examined in some detail the mechanisms by which the hRNR (both β’ and β) and *L. leichmannii* RNR are inactivated by F_2CDP or F_2CTP (18,37). They

share many striking similaries despite the difference in cofactor requirement and quaternary structures. In all cases, despite stoichiometric inactivation, multiple pathways are required to account for the observed results. The mechanism by which F_2CDP inactivates RNR *in vivo* remains to be unraveled. However, it is likely that the alkylative pathway is the mechanism involved given the availability of reductants. The tight complex formed between the two subunits of the class I RNRs after incubation with F_2CDP and our ability to radiolabel the sugar moiety of F_2CDP that ends up covalently bound to the protein, may allow us to assess if similar chemistry is occurring inside the cell.

Acknowledgments

We thank Joey Cotruvo in our lab for his thoughtful comments.

Abbreviations

RNR	ribonucleotide reductase
α	ribonucleotide reductase large subunit
β	ribonucleotide reductase small subunit
hRNR	human RNR
dNDP	deoxynucleoside 5′-diphosphate
NDP	nucleoside 5′-diphosphate
DTT	1,4-dithiothreitol
eq.	equivalents
β-ME	β-mercaptoethanol
TR	thioredoxin
TRR	thioredoxin reductase
SA	specific activity
wt	wild type
TEAB	triethylammonium bicarbonate
hdCK	human deoxycytidine kinase
hCMPK	human UMP/CMP kinase
Y•	tyrosyl radical
GST-CMK	glutathione S-transferase fusion to human UMP/CMP kinase
F_2C	2′, 2′-dideoxy-difluorocytidine or gemcitabine
F_2CDP	5′-diphosphate of F_2C
F_2CTP	5′-triphosphate of F_2C
Buffer A	50 mM HEPES pH 7.6, 15 mM $MgSO_4$, 1 mM EDTA

REFERENCES

1. Hertel LW, Boder GB, Kroin JS, Rinzel SM, Poore GA, Todd GC, Grindey GB. Evaluation of the antitumor-activity of gemcitabine (2′,2′-difluoro-2′-deoxycytidine). Cancer Res 1990;50:4417–4422. [PubMed: 2364394]

2. Huang P, Chubb S, Hertel LW, Grindey GB, Plunkett W. Action of 2′,2′-difluorodeoxycytidine on DNA-synthesis. Cancer Res 1991;51:6110–6117. [PubMed: 1718594]

3. Plunkett W, Huang P, Gandhi V. Gemcitabine: actions and interactions. Nucleosides & nucleotides 1997;16:1261–1270.

4. Davidson JD, Ma L, Flagella M, Geeganage S, Gelbert LM, Slapak CA. An increase in the expression of ribonucleotide reductase large subunit 1 is associated with gemcitabine resistance in non-small cell lung cancer cell lines. Cancer Res 2004;64:3761–3766. [PubMed: 15172981]

5. Duxbury M, Ito H, Zinner MJ, Ashley SW, Whang EE. RNA interference targeting the M2 subunit of ribonucleotide reductase enhances pancreatic adenocarcinoma chemosensitivity to gemcitabine. Oncogene 2004;23:1539–1548. [PubMed: 14661056]

6. Arner ES, Eriksson S. Mammalian deoxyribonuclease kinases. Pharmacology & therapeutics 1995;67:155–186. [PubMed: 7494863]

7. Hsu SH, Liou JY, Dutschman GE, Cheng YC. Phosphorylation of cytidine, deoxycytidine, and their analog monophosphates by human UMP/CMP kinase is differentially regulated by ATP and magnesium. Mol Pharmacol 2005;67:806–814. [PubMed: 15550676]

8. Van Rompay AR, Johansson M, Karlsson A. Phosphorylation of deoxycytidine analog monophosphates by UMP-CMP kinase: molecular characterization of the human enzyme. Mol. Pharmacol 1999;56:562–569. [PubMed: 10462544]

9. Cheng YC, Agarwal RP, Parks RE Jr. Erythrocytic nucleoside diphosphokinase. IV. Evidence for electrophoretic heterogeneity. Biochemistry 1971;10:2139–2143. [PubMed: 5562833]

10. Stubbe J, van der Donk WA. Ribonucleotide reductases: radical enzymes with suicidal tendencies. Chem. Biol 1995;12:793–801. [PubMed: 8807812]

11. Stubbe J, van der Donk WA. Protein radicals in enzyme catalysis. Chem. Rev 1998;98:705–762. [PubMed: 11848913]

12. Gandhi V, Plunkett W. Modulatory activity of 2′, 2′-difluorodeoxycytidine on the phosphorylation and cytotoxicity of arabinosyl nucleosides. Cancer Res 1990;50:3675–3680. [PubMed: 2340517]

13. Heinemann V, Xu YZ, Chubb S, Sen A, Hertel LW, Grindey GB, Plunkett W. Inhibition of ribonucleotide reduction in Ccrf-Cem cells by 2′,2′-difluorodeoxycytidine. Mol. Pharmacol 1990;38:567–572. [PubMed: 2233693]

14. Gandhi V, Huang P, Xu YZ, Heinemann V, Plunkett W. Metabolism and action of 2′,2′-difluorodeoxycytidine: self-potentiation of cytotoxicity. Adv Exp Med Biol 1991;309A:125–130. [PubMed: 1789190]

15. van der Donk WA, Yu GX, Perez L, Sanchez RJ, Stubbe J, Samano V, Robins MJ. Detection of a new substrate-derived radical during inactivation of ribonucleotide reductase from *Escherichia coli* by gemcitabine 5′-diphosphate. Biochemistry 1998;37:6419–6426. [PubMed: 9572859]

16. Baker CH, Banzon J, Bollinger JM, Stubbe J, Samano V, Robins MJ, Lippert B, Jarvi E, Resvick R. 2′-deoxy-2′-methylenecytidine and 2′-deoxy-2′,2′-difluorocytidine 5′-diphosphates - potent mechanism-based inhibitors of ribonucleotide reductase. J. Med. Chem 1991;34:1879–1884. [PubMed: 2061926]

17. Silva DJ, Stubbe J, Samano V, Robins MJ. Gemcitabine 5 ′-triphosphate is a stoichiometric mechanism-based inhibitor of *Lactobacillus leichmannii* ribonucleoside triphosphate reductase: Evidence for thiyl radical-mediated nucleotide radical formation. Biochemistry 1998;37:5528–5535. [PubMed: 9548936]

18. Wang J, Lohman GJ, Stubbe J. Enhanced subunit interactions with gemcitabine-5′-diphosphate inhibit ribonucleotide reductases. Proc. Natl. Acad. Sci. U S A 2007;104:14324–14329. [PubMed: 17726094]

19. Cerqueira NM, Fernandes PA, Ramos MJ. Understanding ribonucleotide reductase inactivation by gemcitabine. Chem. Eur. J 2007;13:8507–8515.

20. Pereira S, Fernandes PA, Ramos MJ. Mechanism for ribonucleotide reductase inactivation by the anticancer drug gemcitabine. J Comput Chem 2004;2004:1286–1294. [PubMed: 15139041]

21. Mao SS, Holler TP, Yu GX, Bollinger JM, Booker S, Johnston MI, Stubbe J. A model for the role of multiple cysteine residues involved in ribonucleotide reduction - amazing and still confusing. Biochemistry 1992;31:9733–9743. [PubMed: 1382592]

22. Mao SS, Holler TP, Bollinger JM Jr, Yu GX, Johnston MI, Stubbe J. Interaction of C225SR1 mutant subunit of ribonucleotide reductase with R2 and nucleoside diphosphates: tales of a suicidal enzyme. Biochemistry 1992;31:9744–9751. [PubMed: 1390750]
23. Zipse H, Artin E, Wnuk S, Lohman GJ, Martino D, Griffin RG, Kacprzak S, Kaupp M, Hoffman B, Bennati M, Stubbe J, Lees N. Stucture of the nucleotide radical formed during reaction of CDP/TTP with the E441Q-α2β2 of *E. coli* ribonucleotide reductase. J. Am. Chem. Soc 2009;131:200–211. [PubMed: 19128178]
24. Lohman, GJS.; Stubbe, J. Inactivation of *Lactobacillus leichmannii* ribonucleotide reductase by F_2CTP: covalent modification (part I). 2009. manuscript in preparation for Biochemistry
25. Lohman, GJS.; Gerfen, GJ.; Stubbe, J. Inactivation of *L. leichmannii* ribonucleotide reductase by F_2CTP: adenosylcobalamin destruction and formation of a nucleotide based radical. 2009. manuscript in preparation for Biochemistry
26. Ge J, Yu GX, Ator MA, Stubbe J. Pre-steady-state and steady-state kinetic analysis of *E. coli* class I ribonucleotide reductase. Biochemistry 2003;42:10071–10083. [PubMed: 12939135]
27. Yee CS, Seyedsayamdost MR, Chang MCY, Nocera DG, Stubbe J. Generation of the R2 subunit of ribonucleotide reductase by intein chemistry: insertion of 3-nitrotyrosine at residue 356 as a probe of the radical initiation process. Biochemistry 2003;42:14541–14552. [PubMed: 14661967]
28. Bollinger JMJ, Tong WH, Ravi N, Huynh BH, Edmondson DE, Stubbe JA. Use of rapid kinetics methods to study the assembly of the diferric-tyrosyl radical cofactor of *E. coli* ribonucleotide reductase. Methods Enzymol 1995;258:278–303. [PubMed: 8524156]
29. Lunn CA, Kathju S, Wallace BJ, Kushner SR, Pigiet V. Amplification and purification of plasmid-encoded thioredoxin from *Escherichia coli* K12. J. Biol. Chem 1984;259:469–474.
30. Russel M, Model P. Direct cloning of the trxB gene that encodes thioredoxin reductase. J. Bacteriol 1985;163:238–242. [PubMed: 2989245]
31. Rylova SN, Albertioni F, Flygh G, Eriksson S. Activity profiles of deoxynucleoside kinases and 5′-nucleotidases in cultured adipocytes and myoblastic cells: insights into mitochondrial toxicity of nucleoside analogs. Biochem Pharmacol 2005;69:951–960. [PubMed: 15748706]
32. Steeper JR, Steuart CC. A rapid assay for CDP reductase activity in mammalian cell extracts. Anal. Biochem 1970;34:123–130. [PubMed: 5440901]
33. Bennati M, Farrar CT, Bryant JA, Inati SJ, Weis V, Gerfen GJ, Riggs-Gelasgo P, Stubbe J, Griffin RG. Pulsed electron-nuclear double resonance (ENDOR) at 140 GHz. J Magn Res 1999;138:232–243.
34. Lawrence CC, Bennati M, Obias HV, Barr G, Griffin RG, Stubbe J. High-field EPR detection of a disulfide radical anion in the reduction of cytidine 5′-diphosphate by the E441Q R1 mutant of *Escherichia coli* ribonucleotide reductase. Proc. Natl. Acad. Sci. U S A 1999;96:8979–8984. [PubMed: 10430881]
35. Stoll S, Schweiger A. A comprehensive software package for spectral simulation and analysis in EPR. J. Magn. Reson 2006;178:42–55. [PubMed: 16188474]
36. Climent I, Sjöberg BM, Huang CY. Site-directed mutagenesis and deletion of the carboxyl terminus of *Escherichia coli* ribonucleotide reductase protein R2-effects on catalytic activity and subunit Interaction. Biochemistry 1992;31:4801–4807. [PubMed: 1591241]
37. Wang, J.; Lohman, GJ.; Stubbe, J. Mechanism of inactivation of human ribonucleotide reductase with p53R2 by gemcitabine-5′-diphosphate. 2009. submitted to Biochemistry
38. Stubbe J, Kozarich JW. Fluoride, pyrophosphate, and base release from 2′-deoxy-2′-fluoronucleoside 5′-diphosphates by ribonucleoside-diphosphate reductase. J. Biol. Chem 1980;255:5511–5513. [PubMed: 6247337]
39. Xu H, F. C, Uchiki T, Fairman JW, Racca J, Dealwis C. Structures of eukaryotic ribonucleotide reductase I provide insights into dNTP regulation. Proc. Natl. Acad. Sci. U S A 2006;103:4022–4027. [PubMed: 16537479]

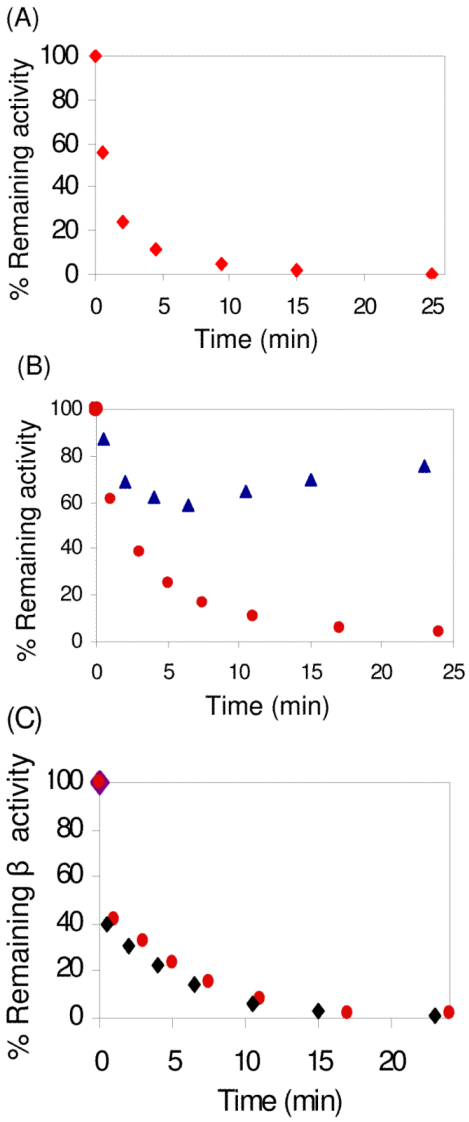

Figure 1.

Time-dependent inactivation of *E. coli* wt-RNR (3 μM) or C225S-RNR by F_2CDP (3 or 6 μM) in the absence of reductant, assayed by Method 1 or Method 2. **A**. Method 1: inactivation mixture diluted 10-fold with 1 F_2CDP/α2; **B**. α (▲) and β (●) inactivation mixture diluted 20-fold in the presence of a 5-fold excess of the second subunit and 6 μM F_2CDP; **C**. Method 2 as in **B** except C225S-RNR replaced wt-RNR. The remaining β activity was assayed in the absence of reductant (●) and in the presence of reductant (DTT, ◆).

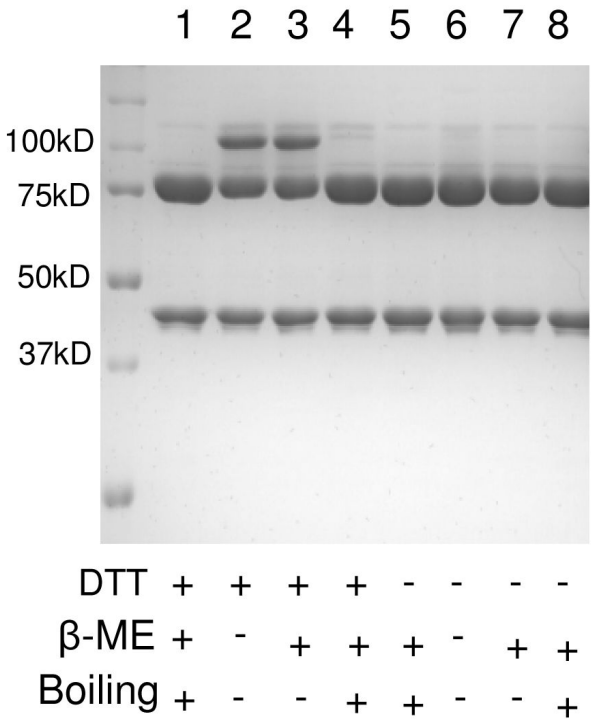

Figure 2.
SDS-PAGE (10%) analysis of the α/β complex (5 μM) inactivated by F_2CDP (12.5 μM) and ATP (3 mM) in the presence or in the absence of DTT at 25 °C for 5 min. Each sample was mixed with 2× loading buffer ± β-ME, +/− boiling for 2 min before loading as indicated. A band at 110 kDa is observed in Lanes 2, 3 (inactivation in the presence of DTT, without boiling).

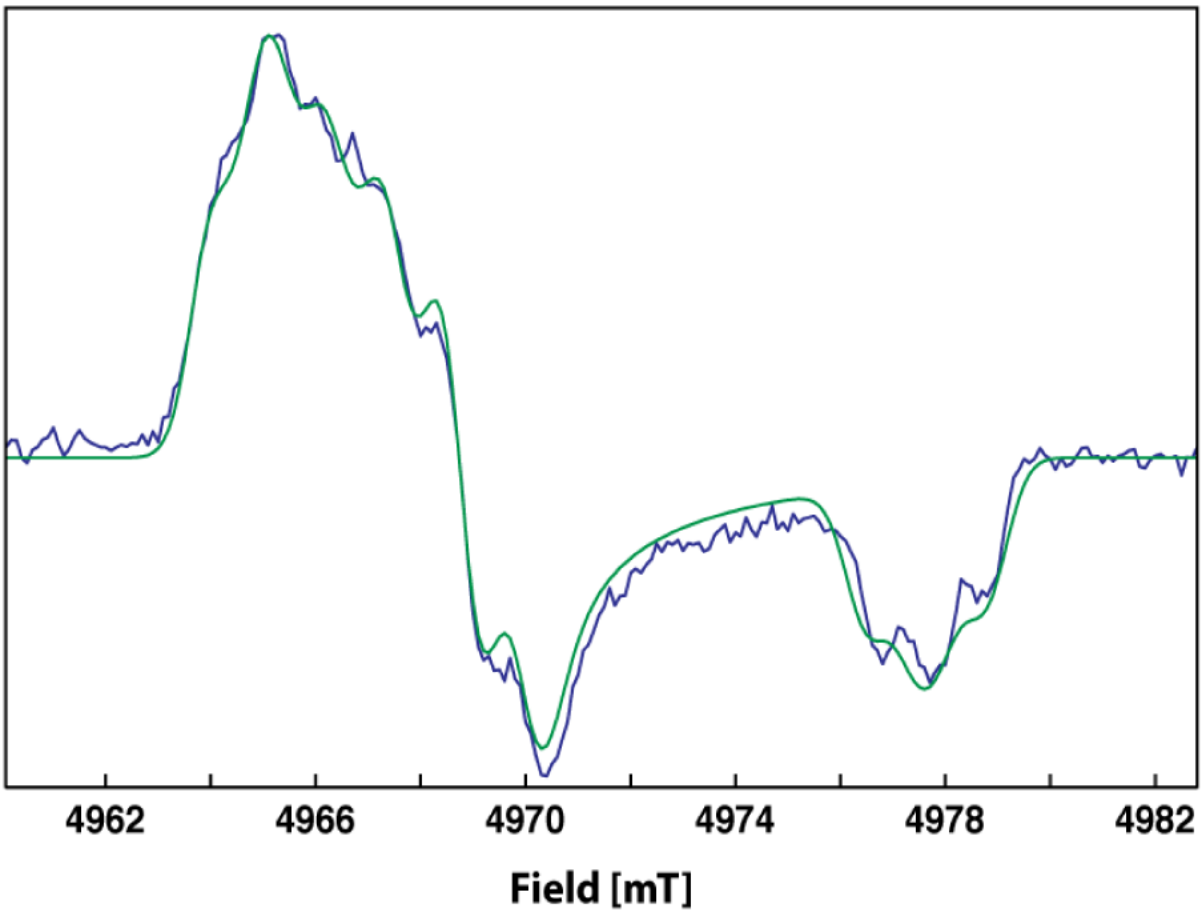

Figure 3.

Echo-detected 139.5 GHz EPR spectrum of F_2CDP-inactivated RNR recorded at 65 K. 1000 shots were accumulated for each point in the spectrum. The stimulated echo pulse width was $t_{\pi/2}$=56 ns and t_p=200 ns. g-values obtained from the spectrum are as follows: g_x=2.00738, g_y=2.00592, g_z=2.00230. Two hyperfine couplings were used in the simulation with A_1= (11.4, 14.6, 12.8) and A_2=(8.5, 8.5, 8.5).

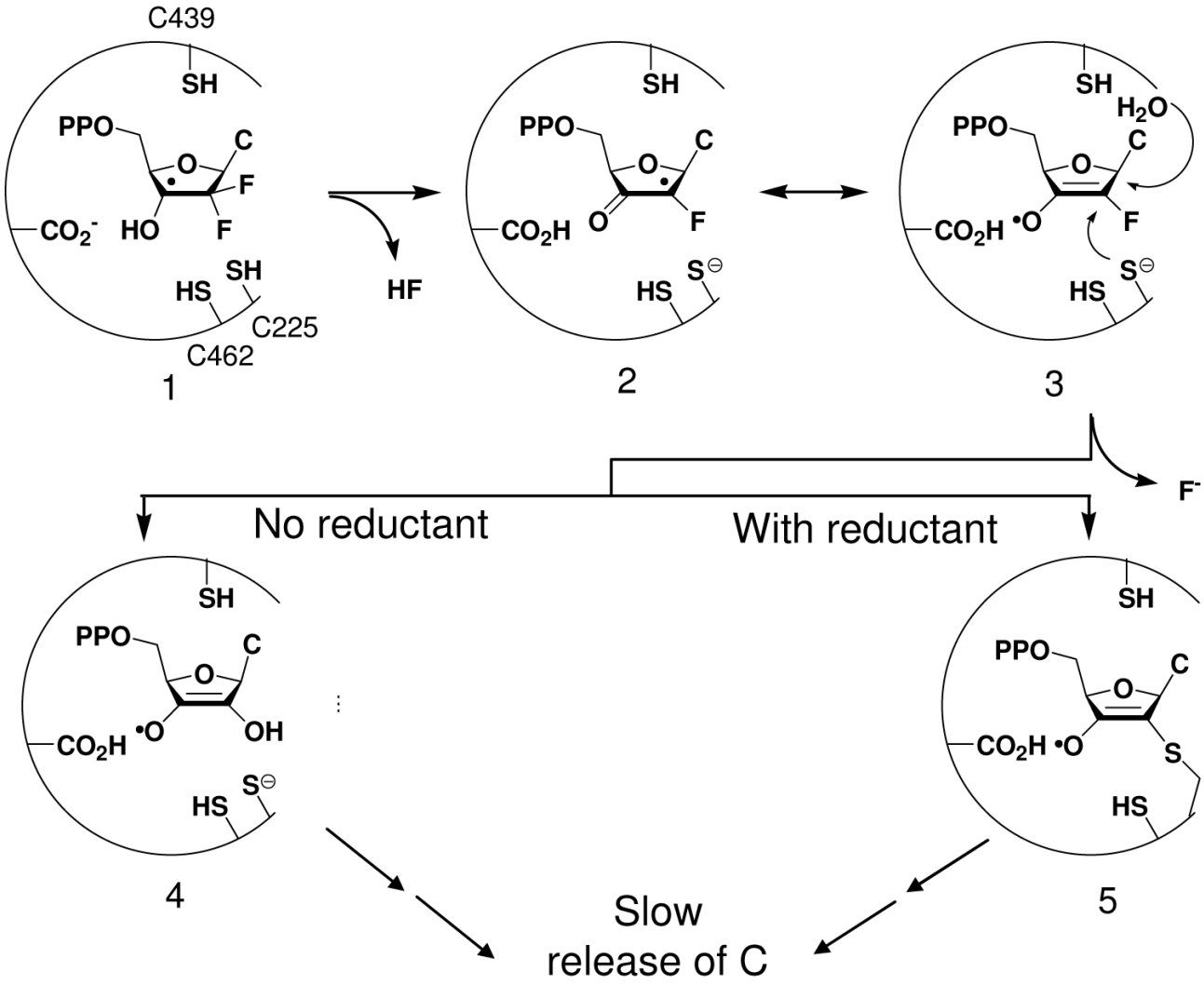

Figure 4.
Proposed mechanism of inactivation of RNR by F_2CDP in the absence (**4**) and the presence (**5**) of reductant.

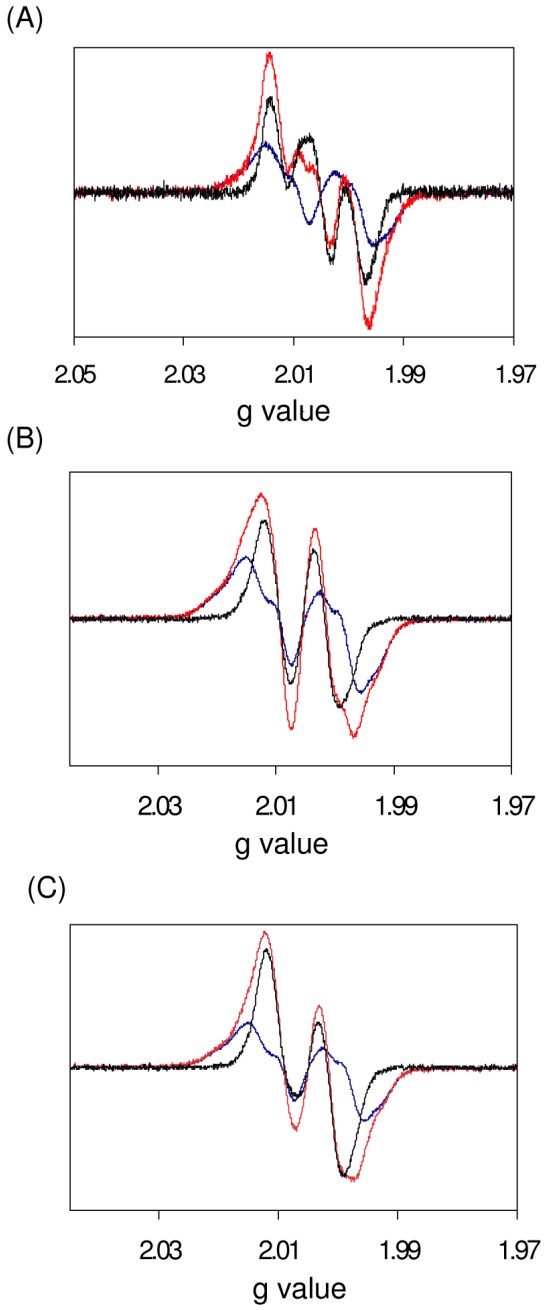

Figure 5.

EPR Spectrum at 9 GHz of *E. coli* wt-RNR (15 μM) or C225S-RNR (15 μM) inactivated by F_2CDP or [1′-^{2}H] F_2CDP. **A**. The reaction mixture with F_2CDP was frozen in liquid N_2 at 45 s (red) and is a composite of Y• and new radical. The Y• (blue) was subtracted from the red spectrum to give the black spectrum of the new radical. **B**. As in **A** except that [1′-^{2}H] F_2CDP replaced F_2CDP. **C**. As in A. except that C225S RNR and [1′-^{2}H] F_2CDP replaced wt-RNR and F_2CDP.